



Study of Dark Energy Stars in a Buchdahl Spacetime

Manuel Malaver

Maritime University of the Caribbean, Department of Basic Sciences, Catia la Mar, Venezuela.

Abstract

In this paper we obtained some spherically stellar configurations that represent new models of dark energy stars specifying particular forms for gravitational potential and the electric field intensity which allows solve the Einstein-Maxwell field equations. We have chosen the metric potential proposed by Buchdahl (1959) with the equation of state $p_r = \omega \rho$ where p_r is the radial pressure, ρ is the dark energy density and ω is the dark energy parameter. We found that the radial pressure, the anisotropy factor, energy density, metric coefficients, mass function, charge density are regular and well behaved in the stellar interior but the causality conditions and of strong energy are not satisfied. These models have great application in physics and cosmology due to the fact that several independent observations indicate that the universe is in a phase of accelerated expansion which can be explained by the presence of dark energy that has not been detected.

Keywords: Dark Energy Stars, Metric Potential, Causality Condition, Strong Energy Condition, Accelerated Expansion.

INTRODUCTION

Recent observational evidence as measurements of supernovas of type Ia and microwave background radiation suggest a accelerate expansion of the universe [1] and the explanation for this cosmological behavior requires assuming that a considerable part of the universe consists of a hypothetical dark energy with a negative pressure component [2], which is a cosmic fluid parameterized by an equation of state $\omega = p/\rho < -1/3$ where p is the spatially homogeneous pressure and ρ the dark energy density [1-4]. The range for which $\omega < -1$ has been denoted phantom energy and possesses peculiar properties, such as negative temperatures and the energy density increases to infinity in a finite time, resulting in a big rip [2-4]. It also provides a natural scenario for the existence of exotic geometries such as wormholes [5-7].

The notion of dark energy is that of a homogeneously distributed cosmic fluid and when extended to inhomogeneous spherically symmetric spacetimes, the pressure appearing in the equation of state is now a negative radial pressure, and the tangential pressure is then determined via the field equations [8,9]. Lobo [9] explored several configurations, by imposing specific choices for the mass function and studied the dynamical stability of these models by applying the general stability formalism developed by Lobo and Crawford [10]. Chan et al. [14] propose that the mass function is a natural consequence of the Einstein's field equations and considered a core with a homogeneous energy density, described by the Lobo's first solution [9]. Malaver and Esculpi [11] presented a new model of dark energy star by imposing specific choice for the mass function that correspond an increase in energy density inside of the star. Bibi et al. [12] obtained a new class of solutions of

the Einstein-Maxwell field equations which represents a model for dark energy stars with the equation of state $p_r = -\rho$. Malaver et al. [13] found a new family of solutions to the Einstein-Maxwell system considering a particular form of the gravitational potential $Z(x)$ and the electric field intensity with a linear equation of state that represents a model of dark energy star. Malaver and Kasmaei [14] generated a dark energy star model with a quadratic equation of state and a specific charge distribution. According Chan et al. [15] the denomination dark energy is applied to fluids which violate only the strong energy condition (SEC) given by $\rho + p_r + 2p_t \geq 0$ where ρ is the energy density, p_r and p_t are the radial pressure and tangential pressure, respectively.

The analysis of compact objects with anisotropic matter distribution is very important, because that the anisotropy plays a significant role in the studies of relativistic spheres of fluid [16-30]. Anisotropy is defined as $\Delta = p_t - p_r$ where p_r is the radial pressure and p_t is the tangential pressure. The existence of solid core, presence of type 3A superfluid [31], magnetic field, phase transitions, a pion condensation and electric field [30] are most important reasonable facts that explain the presence of tangential pressures within a star. Many astrophysical objects as X-ray pulsar, Her X-1, 4U1820-30 and SAXJ1804.4-3658 have anisotropic pressures. Bowers and Liang [32] include in the equation of hydrostatic equilibrium the case of local anisotropy. Feroze and Siddiqui [33], Malaver [34-35] and Sunzu et al. [23] obtained solutions of the Einstein-Maxwell field equations for charged spherically symmetric space-time by assuming anisotropic pressure. Bhar et al. [36] have studied the behavior of relativistic objects with locally anisotropic matter distribution considering the Tolman VII form for the gravitational potential with a linear relation between the energy density and the radial pressure.

EINSTEIN-MAXWELL FIELD EQUATIONS

Several mathematical modeling within the framework of the general theory of relativity has been used to explain the behavior and structure of massive objects as neutron stars, quasars, black holes, pulsars and white dwarfs [1,2] and requires finding the exact solutions of the Einstein-Maxwell system [3]. A detailed and systematic analysis was carried out by Delgaty and Lake [4] which obtained several analytical solutions that can describe realistic stellar configurations.

We consider a spherically symmetric, static and homogeneous spacetime. In Schwarzschild coordinates the metric is given by

$$ds^2 = -e^{2\nu(r)} dt^2 + e^{2\lambda(r)} dr^2 + r^2(d\theta^2 + \sin^2\theta d\phi^2) \quad (1)$$

where $\nu(r)$ and $\lambda(r)$ are two arbitrary functions.

Recently, astronomical observations of compact objects have allowed new findings of neutron stars and strange stars that adjust to the exact solutions of the 4-D Einstein field equations and the data on mass maximum, redshift and luminosity are some of the most relevant characteristics for verifying the physical requirements of these models [37]. A great number of exact models from the Einstein-Maxwell field equations have been generated by Mafa Takisa and Maharaj [18], Malaver and Kasmaei [14], Malaver [19,20], Ivanov [22] and Sunzu et al [23]. In the development of these models, several forms of equations of state can be considered [24]. Komathiraj and Maharaj [25], Malaver [26], Bombaci [27], Thirukkanesh and Maharaj [28], Dey et al. [29] and Usov [30] assume linear equation of state for quark stars. Feroze and Siddiqui [33] considered a quadratic equation of state for the matter distribution and specified particular forms for the gravitational potential and electric field intensity. Mafa Takisa and Maharaj [18] obtained new exact solutions to the Einstein-Maxwell system of equations with a polytropic equation of state. Thirukkanesh and Ragel [38] have obtained particular models of anisotropic fluids with polytropic equation of state which are consistent with the reported experimental observations. Malaver [39] generated new exact solutions to the Einstein-Maxwell system considering Van der Waals modified equation of state with polytropic exponent. Tello-Ortiz et al. [40] found an anisotropic fluid sphere solution of the Einstein-Maxwell field equations with a modified version of the Chaplygin equation of state. More recently, Prasad et al. [41] proposed a new model of an anisotropic compact star which admits the Chaplygin equation of state considering the metric potential of Buchdahl [42].

The Einstein field equations for the charged anisotropic matter are given by

$$\frac{1}{r^2}(1 - e^{-2\lambda}) + \frac{2\lambda'}{r} e^{-2\lambda} = \rho + \frac{1}{2} E^2 \quad (2)$$

$$-\frac{1}{r^2}(1 - e^{-2\lambda}) + \frac{2\nu'}{r} e^{-2\lambda} = p_r - \frac{1}{2} E^2 \quad (3)$$

$$e^{-2\lambda} \left(\nu'' + \nu'^2 + \frac{\nu'}{r} - \nu \lambda' - \frac{\lambda'}{r} \right) = p_t + \frac{1}{2} E^2 \quad (4)$$

$$\sigma = \frac{1}{r^2} e^{-\lambda} (r^2 E)'$$

where ρ is the energy density, p_r is the radial pressure, E is electric field intensity,

p_t is the tangential pressure and primes denote differentiations with respect to r. Using the transformations, $x = cr^2$, $Z(x) = e^{-2\lambda(r)}$ and $A_2y_2(x) = e^{2\nu(r)}$ with arbitrary constants A and $c > 0$, suggested by Durgapal and Bannerji [43], the Einstein field equations can be written as

$$\frac{1-Z}{x} - 2\dot{Z} = \frac{\rho}{c} + \frac{E^2}{2c} \quad (6)$$

$$4xZ\dot{y} - \frac{1-Z}{x} = \frac{p_r}{c} - \frac{E^2}{2c} \quad (7)$$

$$4xZ\ddot{y} + (4Z + 2x\dot{Z})\dot{y} + \dot{Z} = \frac{p_t}{c} + \frac{E^2}{2c} \quad (8)$$

$$p_t = p_r + \Delta \quad (9)$$

$$\frac{\Delta}{c} = 4xZ\ddot{y} + \dot{Z} \left(1 + 2x\frac{\dot{y}}{y} \right) + \frac{1-Z}{x} - \frac{E^2}{c} \quad (10)$$

$$\sigma^2 = \frac{4cZ}{x} (x\dot{E} + E)^2 \quad (11)$$

σ is the charge density, $\Delta = p_t - p_r$ is the anisotropic factor and dots denote differentiation with respect to x. With the transformations of [43], the mass within a radius r of the sphere takes the form

$$m(x) = \frac{1}{4c^{3/2}} \int_0^x \sqrt{x} (\rho^* + E^2) dx \quad (12)$$

where

$$\rho^* = \left(\frac{1-Z}{x} - 2\dot{Z} \right) c$$

The interior metric (1) with the charged matter distribution should match the exterior spacetime described by the Reissner-Nordstrom metric:

$$ds^2 = -\left(1 - \frac{2M}{r} + \frac{Q^2}{r^2} \right) dt^2 + \left(1 - \frac{2M}{r} + \frac{Q^2}{r^2} \right) dr^2 + r^2(d\theta^2 + \sin^2\theta d\phi^2) \quad (13)$$

where the total mass and the total charge of the star are denoted by M and q^2 , respectively. The junction conditions at the stellar surface are obtained by matching the first and the second fundamental forms for the interior metric (1) and the exterior metric (13).

In this paper, we assume the following equation of state

$$p_r = \omega\rho \quad (14)$$

The aim of this paper is to generate new class of solutions which represents a potential model of dark energy stars whose equation of state is $p_r = \omega\rho$ with anisotropic matter distribution, specifying particular forms for the gravitational potential and the electric field intensity. We have used the ansatz proposed by Buchdahl [42]. The system of field equations has been solved to obtain analytic solutions which are physically acceptable. We assume that the denominator dark energy is applied to fluids which violate the strong energy condition [15]. This article is organized as follows, in Section 2, we present Einstein's field equations. In Section 3, we make a particular choice of gravitational potential $Z(x)$ that allows solving the field equations and we have obtained new models for dark energy stars consistent alone of dark matter. In Section 4, a physical analysis of the new solutions is performed. Finally in Section 5, we conclude.

where ω is the dark energy parameter.

A NEW CLASS OF MODELS

In order to solve the Einstein field equations, we have chosen specific forms for the gravitational potential $Z(x)$ and the electrical field intensity E . Following Buchdahl [42] and Ngubelanga et al.[44] we have taken the forms, respectively

$$Z(x) = \frac{K+x}{K(1+x)} \tag{15}$$

$$\frac{E^2}{2c} = x(a+bx) \tag{16}$$

where K is a parameter related to the geometry of the star and a, b are real constants. The metric potential is regular at the origin and well behaved in the interior of the sphere. The electric field is finite at the center of the star and remains continuous in the interior.

Substituting (15) and (16) in (7) we obtain

$$\rho = \frac{c[(K-1)(x+3) - Kx(a+bx)(x+1)^2]}{K(x+1)^2} \tag{17}$$

Replacing (17) in (14), we have for the radial pressure

$$P_r = \frac{\omega c[(K-1)(x+3) - Kx(a+bx)(x+1)^2]}{K(x+1)^2} \tag{18}$$

Using (17) in (12), the expression of the mass function is

$$M(x) = x^{3/2} \frac{[-5Kbx^3 - (7a+5b)Kx^2 - 7Kax + 35K - 35]}{70K\sqrt{c}(x+1)} \tag{19}$$

With (15) and (16) in (11), the charge density is

$$\sigma^2 = \frac{2c^2(K+x)(4bx+3a)^2}{K(x+1)(a+bx)} \tag{20}$$

With (15), (16) and (17), the eq. (8) becomes

$$\frac{4(K+x)}{(1+x)} \frac{y}{y'} = \frac{(K-1)}{K(1+x)} - x(a+bx) + \omega \frac{[(K-1)(x+3) - Kx(a+bx)(x+1)^2]}{K(x+1)^2} \tag{21}$$

Integrating (21), we obtain

$$y(x) = c_1(x+1)^A (K+x)^B e^{\frac{(\omega+1)[Cx^3+Dx^2+Ex]}{24}} \tag{22}$$

where

$$A = \frac{1}{2}\omega \tag{23}$$

$$B = \frac{(\omega+1)[bK^4 - (a+b)K^3 + aK^2 + K] - (3\omega+1)}{4} \tag{24}$$

$$C = -2bK \tag{25}$$

$$D = 3K[bK - (a+b)] \tag{26}$$

$$E = 6K[-bK^2 + (a+b)K - a] \tag{27}$$

The metric functions can be written as

$$e^{2\lambda(r)} = \frac{K(1+x)}{K+x} \tag{28}$$

$$e^{2\nu(r)} = A^2 c_1^2 (x+1)^{2A} (K+x)^{2B} e^{\frac{(\omega+1)[Cx^3+Dx^2+Ex]}{12}} \tag{29}$$

The anisotropy factor Δ is given by for

$$\Delta = \frac{4xc(K+x)}{K(1+x)} + \frac{B(\omega+1)(3Cx^2+2Dx+E)}{12(K+x)} + \frac{(\omega+1)(6Cx+2D)}{24} + \frac{(\omega+1)^2(3Cx^2+2Dx+E)^2}{576} + \frac{(1-K)c}{K(1+x)^2} \left[1 + 2x \left(\frac{A}{x+1} + \frac{B}{K+x} + \frac{(\omega+1)(3Cx^2+2Dx+E)}{24} \right) \right] + \frac{c(K-1)}{K(1+x)} - 2xc(a+bx) \tag{30}$$

CONDITIONS OF PHYSICAL ACCEPTABILITY

For a model to be physically acceptable, the following conditions should be satisfied [4,38]:

(i) The metric potentials $e^{2\lambda}$ and $e^{2\nu}$ assume finite values throughout the stellar interior and are singularity-free at the center $r=0$.

(ii) The energy density ρ should be positive and a decreasing function inside the star.

(iii) The radial pressure also should be positive and a decreasing function of radial parameter but for negative pressure this condition is not satisfied.

(iv) The density gradient $\frac{d\rho}{dr} \leq 0$ for $0 \leq r \leq R$.

(v) The anisotropy is zero at the center $r=0$, i.e. $\Delta(r=0) = 0$.

(vi) Any physically acceptable model must satisfy the causality condition, that is, for the radial sound speed $v_{sr}^2 = \frac{dp_r}{d\rho}$, we should have $0 \leq v_{sr}^2 \leq 1$ but the dark energy case this condition nor is it satisfied.

(vii) The consideration of dark energy is applicable only to fluids that violate the strong energy condition.

(viii) The charged interior solution should be matched with the Reissner-Nordström exterior solution, for which the metric is given by the equation (13).

The conditions (ii) and (iv) imply that the energy density must reach a maximum at the centre and decreasing towards the surface of the sphere.

PHYSICAL ANALYSIS THE NEW MODELS

For the new solutions, metric potentials $e^{2\lambda}$ and $e^{2\nu}$ have finite values and remain positive throughout the stellar interior. At the center $e^{2\lambda(0)} = 1$ and $e^{2\nu(0)} = A^2 c_1^2 K^{2B}$. We show that in $r=0$ $(e^{2\lambda(r)})'_{r=0} = (e^{2\nu(r)})'_{r=0} = 0$ and this makes is possible to verify that the gravitational potentials are regular at the center.

The energy density is positive and well behaved between the center and the surface of the star. In the center $\rho(r=0) = \frac{3c(K-1)}{K}$ and $p_r(r=0) = \frac{3\omega c(K-1)}{K}$, therefore the energy density will be non-negative in $r=0$ and $p_r(r=0) < 0$.

For the density gradient inside the stellar interior, we obtain

$$\frac{d\rho}{dr} = \frac{c \left[2(K-1)cr - 2Kcr(a+bc r^2)(1+cr^2)^2 - 2Kc^2 r^3 b(1+cr^2)^2 - 4Kc^2 r^3 (a+bc r^2)(1+cr^2) \right]}{K(1+cr^2)^3} - \frac{4c^2 \left[(K-1)(3+cr^2) - Kcr^2(a+bc r^2)(1+cr^2)^2 \right] r}{K(1+cr^2)^3} \tag{31}$$

On the boundary $r=R$, the solution must match the Reissner-Nordström exterior space-time as:

$$ds^2 = -\left(1 - \frac{2M}{r} + \frac{Q^2}{r^2}\right) dt^2 + \left(1 - \frac{2M}{r} + \frac{Q^2}{r^2}\right)^{-1} dr^2 + r^2 (d\theta^2 + \sin^2 \theta d\phi^2)$$

and therefore, the continuity of e^ν and e^λ across the boundary $r=R$ is

$$e^{2\nu} = e^{-2\lambda} = 1 - \frac{2M}{R} + \frac{Q^2}{R^2} \tag{32}$$

Then for the matching conditions, we obtain:

$$\frac{2M}{R} = \frac{[(K-1) + 2cR^2K(1+cR^2)](a+bcR^2)}{K(1+cR^2)} cR^2 \tag{33}$$

Also in $r=R$ the radial pressure $p_r=0$ and we have

$$bKc^4R^8 + (a+2b)Kc^3R^6 + (2a+b)Kc^2R^4 - (K-1-aK)cR^2 - 3K+3=0 \tag{34}$$

In the figures 1, 2 and 3 are represented the dependence of ρ , $\frac{d\rho}{dr}$ and σ^2 with the radial coordinate for two different values of K . In all the cases was it has been considered $a=0.5$, $b=0.2$, $c=1$.

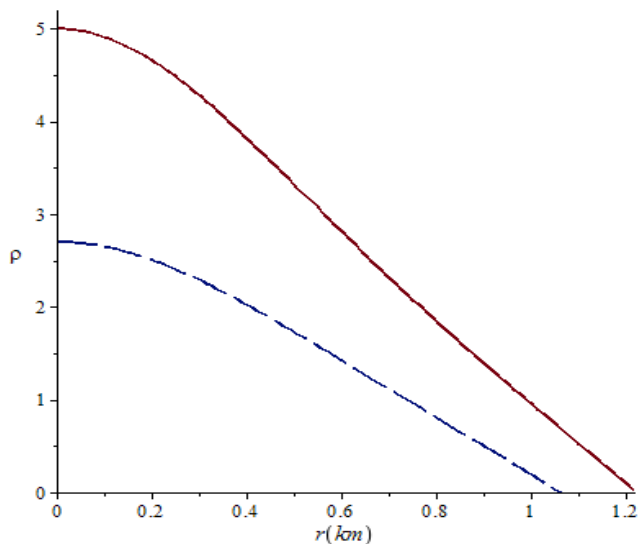


Figure 1. Energy density against radial coordinate for $K=-1.5$ (solid line); $K=10$ (long-dash line) with $a=0.5$, $b=0.2$ and $c=1$.

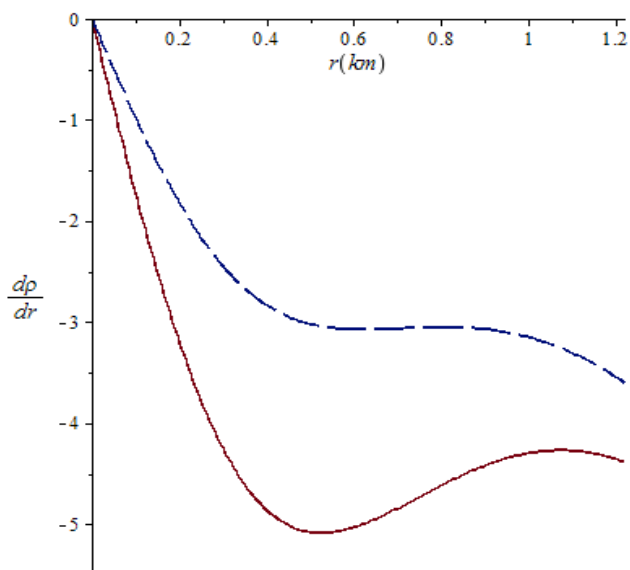


Figure 2. Density gradient against radial coordinate for $K=-1.5$ (solid line); $K=10$ (long-dash line) with $a=0.5$, $b=0.2$ and $c=1$.

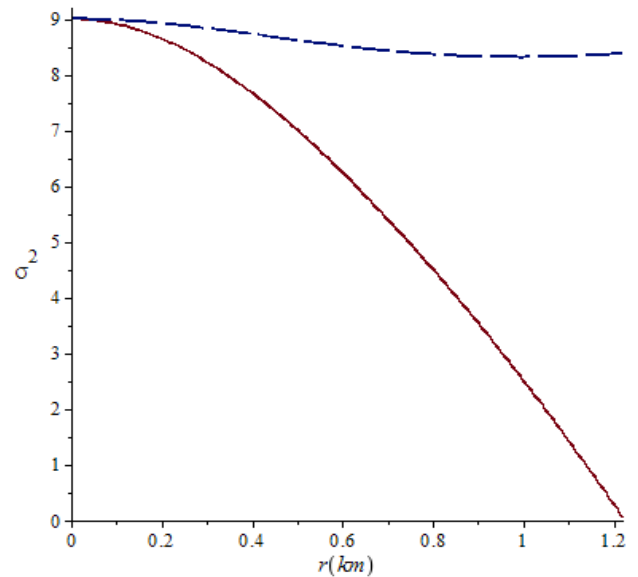


Figure 3. Charge density against radial parameter for $K=-1.5$ (solid line); $K=10$ (long-dash line) with $a=0.5$, $b=0.2$ and $c=1$.

For different values of parameter K , the energy density remains positive, continuous and is monotonically decreasing function throughout the stellar interior as noted in the Figure 1. It is also seen that the density decreases with increasing K . The radial variation of energy density gradient has been shown in Figure 2, in which it is observed that $\frac{d\rho}{dr} < 0$ in the two cases. In the Figure 3 the charge density is a continuously decreasing function inside the star for $K=-1.5$ but for $K=10$ has a small decrease and then slightly increases with the radial parameter.

The Figures 4,5, 6 and 7 show the dependence of $M(r)$, P_r , anisotropy Δ and strong energy condition (SEC) respectively with the radial parameter for $K=-1.5$ and different values of ω . In all the cases it has been considered $a=0.5$, $b=0.2$ and $c=1$.

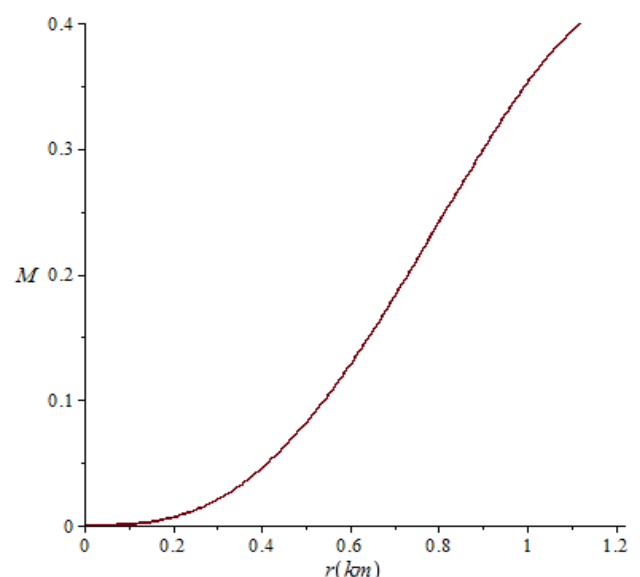


Figure 4. Mass function against radial parameter for $K=-1.5$ with $a=0.5$, $b=0.2$ and $c=1$.

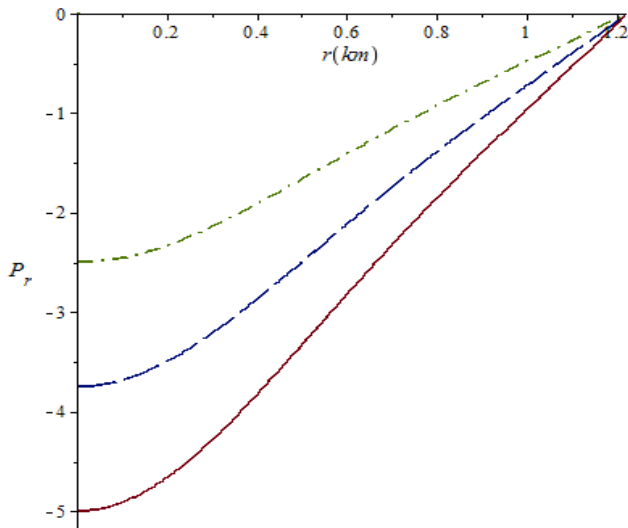


Figure 5. Radial pressure against radial coordinate for $\omega=-1$ (solid line); $\omega=-0.75$ (long-dash line); $\omega=-0.5$ (dashdot line). In all the cases $K=-1.5$ with $a=0.5, b=0.2$ and $c=1$.

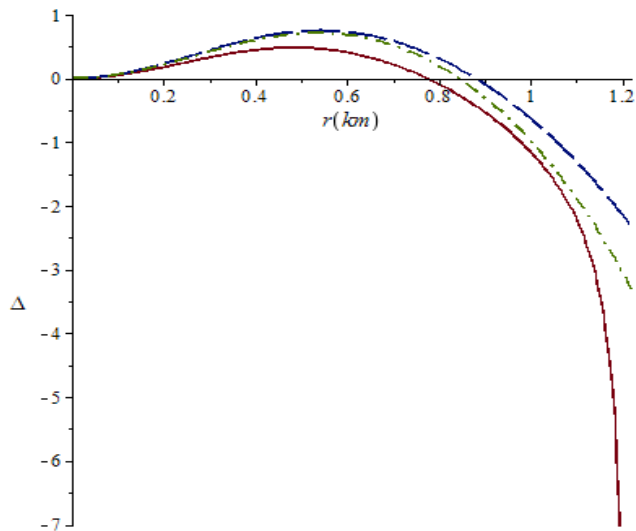


Figure 6. Anisotropy against radial coordinate for $\omega=-1$ (solid line); $\omega=-0.75$ (long-dash line); $\omega=-0.5$ (dashdot line). In all the cases $K=-1.5$ with $a=0.5, b=0.2$ and $c=1$.

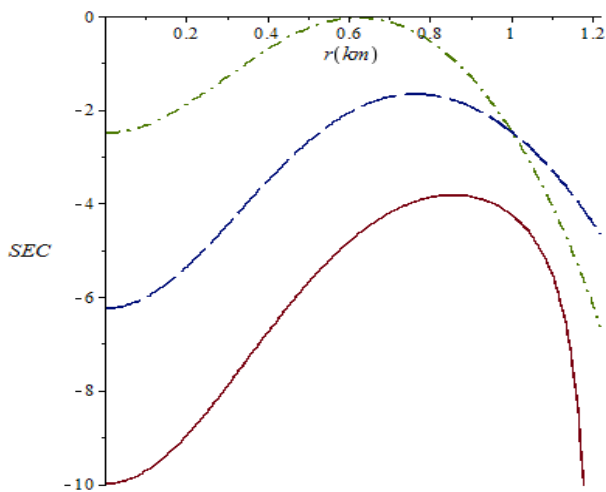


Figure 7. SEC against radial coordinate for $\omega=-1$ (solid line); $\omega=-0.75$ (long-dash line); $\omega=-0.5$ (dashdot line). In all the cases $K=-1.5$ with $a=0.5, b=0.2$ and $c=1$.

In figure 4, the mass function is continuous, strictly increasing and well behaved and the radial pressure is negative and not a decreasing function of the radial parameter but takes higher values when ω is increased as shown in Figure 5. The anisotropic factor is plotted in Figure 6 and it shows that vanishes at the centre of the star, i.e. $\Delta(r=0) = 0$. We can also note that Δ admits higher values with a growth of ω . The Figure 7 shows that the strong energy condition is violated for all ω values considered when $K=-1.5$.

In the figures 8, 9, 10 and 11 has been represented the variation of $M(r)$, P_r , anisotropy Δ and strong energy condition (SEC) with the radial coordinate for the different values of the dark energy parameter ω . In these cases $K=10, a=0.5, b=0.2$ and $c=1$.

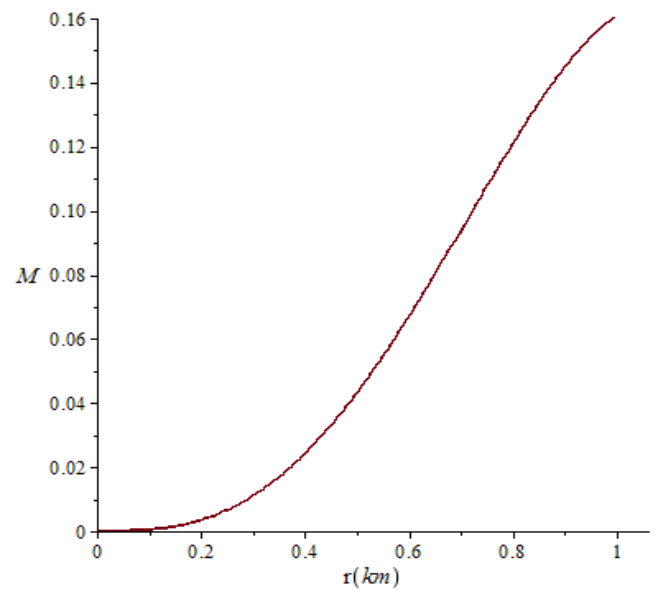


Figure 8. Mass function against radial parameter for $K=10$ with $a=0.5, b=0.2$ and $c=1$.

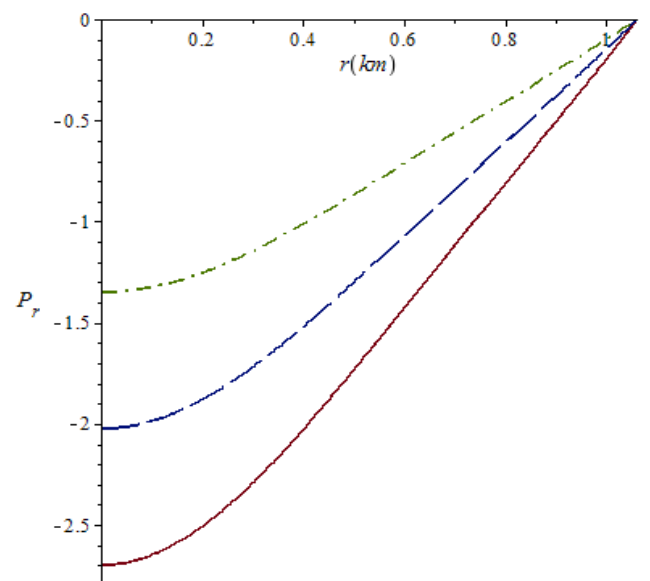


Figure 9. Radial pressure against radial parameter for $\omega=-1$ (solid line); $\omega=-0.75$ (long-dash line); $\omega=-0.5$ (dashdot line). In all the cases $K=10$ with $a=0.5, b=0.2$ and $c=1$.

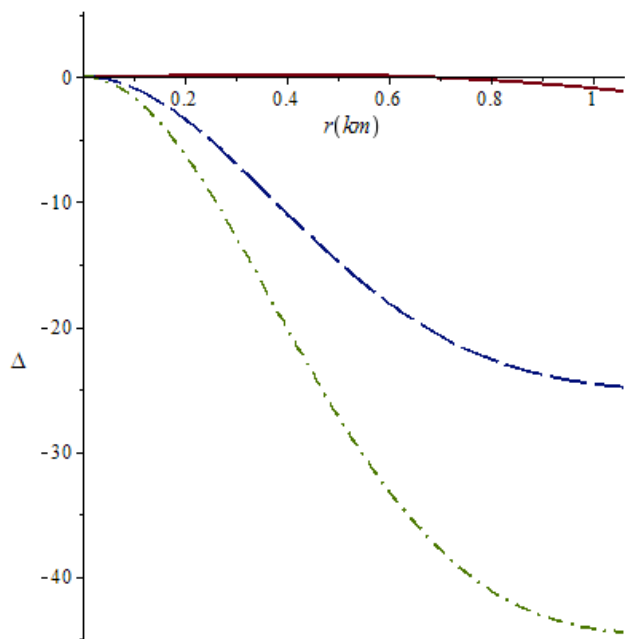


Figure 10. Anisotropy against radial parameter for $\omega=-1$ (solid line); $\omega=-0.75$ (long-dash line); $\omega=-0.5$ (dashdot line). In all the cases $K=10$ with $a=0.5$, $b=0.2$ and $c=1$.

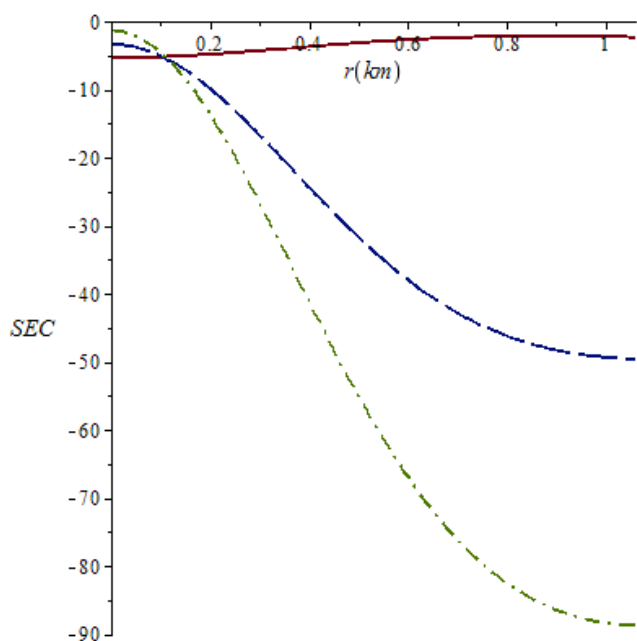


Figure 11. SEC against radial parameter for $\omega=-1$ (solid line); $\omega=-0.75$ (long-dash line); $\omega=-0.5$ (dashdot line). In all the cases $K=10$ with $a=0.5$, $b=0.2$ and $c=1$.

In Figure 8, the mass function also is continuous, increasing, takes finite values and well behaved in the stellar interior and in the Figure 9 the radial pressure is negative at the center $r=0$ and its value grows when ω increases. In Figure 10 the anisotropy also vanishes at the center and decreases for high values of ω . For all ω values considered, the violation of the strong energy condition is satisfied as noted in Figure 11.

CONCLUSION

In this paper we have found new class of solutions which

represents a model for dark energy stars with a gravitational potential proposed for Buchdahl. The radial pressure, energy density, anisotropy, mass function, charge density and all the coefficients of the metric behaves well inside the stellar interior and are free of singularities. In this model, the consideration of dark energy star is applied only to the cases where parameter ω not satisfy the strong energy condition. The obtained solutions match smoothly with the exterior of the Reissner–Nordström spacetime at the boundary $r=R$, because matter variables and the gravitational potentials of this work are consistent with the physical analysis of these stars. The new models satisfy all the requirements for a compact negative energy stellar object and may be used to model relativistic configurations in different astrophysical scenes.

REFERENCES

1. Kuhfitting, P.K.(2011). Some remarks on exact wormhole solutions, *Adv. Stud. Theor. Phys.* 2011, 5, 365.
2. Bicak, J. Einstein equations: exact solutions, *Encyclopaedia of Mathematical Physics.* 2006,2, 165.
3. Malaver, M. Black Holes, Wormholes and Dark Energy Stars in General Relativity. Lambert Academic Publishing, Berlin. ISBN: 978-3-659-34784-9, 2013.
4. Delgaty, M.S.R.; Lake, K. Physical Acceptability of Isolated, Static, Spherically Symmetric, Perfect Fluid Solutions of Einstein's Equations. *Comput. Phys. Commun.* 1998,115, 395.
5. Schwarzschild, K. Uber das Gravitationsfeld einer Kugel aus inkompressibler Flüssigkeit nach der Einsteinschen Theorie. *Math.Phys.Tech.* 1916, 424-434.
6. Morris MS, Thorne KS (1988) Wormholes in spacetime and their use for interstellar travel: A tool for teaching general relativity. *Am J Phys* 56: 395-412.
7. Visser M (1995) Lorentzian wormholes: From Einstein to Hawking. In: 1st (Edn.), AIP Press, New York, USA, pp:412.
8. Lobo FSN (2005) Stability of phantom wormholes. *Phys. Rev D* 71: 124022.
9. Lobo FSN (2006) Stable dark energy stars. *Class Quant Grav* 23: 1525-1541.
10. Lobo FSN, Crawford P (2005) Stability analysis of dynamic thin shells. *Class Quant Grav* 22: 4869- 4886.
11. Malaver M, Esculpi MA (2013) Theoretical Model of Stable Dark Energy Stars. *IJRRAS* 14(1): 26-39.
12. Bibi R, Feroze T, Siddiqui A (2016) Solution of the Einstein-Maxwell Equations with Anisotropic Negative Pressure as a Potential Model of a Dark Energy Star. *Canadian Journal of Physics* 94(8): 758-762.

13. Malaver M, Esculpi M, Govender M (2019) New Models of Dark Energy Stars with Charge Distributions. *International Journal of Astrophysics and Space Science* 7(2): 27-32.
14. Malaver M, Kasmaei HD (2020) Analytical Models of Dark Energy Stars with Quadratic Equation of State. *Applied Physics* 3: 1-14
15. Chan R, da Silva MAF, Villas da Rocha JF (2009) On Anisotropic Dark Energy. *Mod Phys Lett A* 24: 1137-1146.
16. Gupta, Y.K.; Maurya, S.K. A class of charged analogues of Durgapal and Fuloria superdense star. *Astrophys. Space Sci.* 2011, 331, 135-144.
17. Kiess, T.E. Exact physical Maxwell-Einstein Tolman-VII solution and its use in stellar models. *Astrophys. Space Sci.* 2012, 339, 329-338.
18. Mafa Takisa, P.; Maharaj, S.D. Some charged polytropic models. *Gen.Rel.Grav.* 2013, 45, 1951-1969.
19. Malaver, M.; Kasmaei, H.D. Relativistic stellar models with quadratic equation of state. *International Journal of Mathematical Modelling & Computations.* 2020, 10, 111-124.
20. Malaver, M. New Mathematical Models of Compact Stars with Charge Distributions. *International Journal of Systems Science and Applied Mathematics.* 2017, 2, 93-98, DOI: 10.11648/j.ijssam.20170205.13.
21. Malaver, M. Generalized Nonsingular Model for Compact Stars Electrically Charged. *World Scientific News.* 2018, 92, 327-339. Available online: <http://www.worldscientificnews.com/wp-content/uploads/2017/12/WSN-922-2018-327-339.pdf>
22. Ivanov, B.V. Static charged perfect fluid spheres in general relativity. *Phys. Rev.D* 65. 2002, 104011.
23. Sunzu, J.M.; Maharaj, S.D.; Ray, S. Quark star model with charged anisotropic matter. *Astrophysics. Space.Sci.* 2014, 354, 517-524.
24. Sunzu, J.M. Realistic Polytropic Models for Neutral Stars with Vanishing Pressure Anisotropy. *Global Journal of Science Frontier Research: A Physics and Space Science.* 2018, 18, ISSN 2249-4626. <https://journalofscience.org/index.php/GJSFR/article/view/2168>
25. Komathiraj, K.; Maharaj, S.D. Analytical models for quark stars. *Int. J. Mod. Phys.* 2007, D16, 1803-1811.
26. Malaver, M. Analytical models for compact stars with a linear equation of state. *World Scientific News,* 2016, 50, 64-73.
27. Bombaci, I. Observational evidence for strange matter in compact objects from the x-ray burster 4U 1820-30, *Phys. Rev.* 1997, C55, 1587- 1590.
28. Thirukkanesh, S. and Maharaj, S.D. Charged anisotropic matter with a linear equation of state. *Class. Quantum Gravity.* 2008, 25, 235001.
29. Dey, M.; Bombaci, I.; Dey, J.; Ray, S.; Samanta, B.C. Strange stars with realistic quark vector interaction and phenomenological density-dependent scalar potential, *Phys. Lett.* 1998, B438, 123-128.
30. Usov, V. V. Electric fields at the quark surface of strange stars in the color-flavor locked phase. *Phys. Rev. D.* 2004, 70, 067301, DOI: 10.1103/PhysRevD.70.067301.
31. Sokolov, A. I. Phase transitions in a superfluid neutron liquid. *Sov. Phys. JETP.* 1980, 52, 575-576.
32. Bowers, R.L.; Liang, E.P.T. Anisotropic Spheres in General Relativity. *Astrophys. J.* 1974, 188, 657-665.
33. Feroze, T; Siddiqui, A. Charged anisotropic matter with quadratic equation of state. *Gen. Rel. Grav.* 2011, 43, 1025-1035.
34. Malaver, M. Charged anisotropic models in a modified Tolman IV space time. *World Scientific News.* 2018, 101, 31-43.
35. Malaver, M. Charged stellar model with a prescribed form of metric function $\gamma(x)$ in a Tolman VII spacetime. *World Scientific News.* 2018, 108, 41-52.
36. Bhar P; Murad MH.; Pant N. Relativistic anisotropic stellar models with Tolman VII spacetime. *Astrophys Space Sci.* 2015, 359: 13. doi: 10.1007/s10509-015-2462-9.
37. Bhar P, Govender M (2019) Charged compact star model in Einstein-Maxwell-Gauss- gravity. *Astrophys Space Sci* 364: 186.
38. Thirukkanesh, S.; Ragel, F.C. Exact anisotropic sphere with polytropic equation of state. *PRAMANA-Journal of physics.* 2012, 78, 687-696.
39. Malaver, M. Analytical model for charged polytropic stars with Van der Waals Modified Equation of State. *American Journal of Astronomy and Astrophysics.* 2013, 1, 37-42.
40. Tello-Ortiz, F; Malaver, M.; Rincón, A.; Gomez-Leyton, Y. Relativistic Anisotropic Fluid Spheres Satisfying a Non-Linear Equation of State. *Eur. Phys. J. C.* 2020, 80, 371, <https://doi.org/10.1140/epjc/s10052-020-7956-0>.
41. Prasad, A.K., Kumar, J. and Sarkar, A., 2021. Behavior of anisotropic fluids with Chaplygin equation of state in Buchdahl spacetime. *arXiv preprint arXiv:2104.13004*.

42. Buchdahl, H.A., 1959. General relativistic fluid spheres. *Physical Review*, 116(4), p.1027.
43. Durgapal, M.C.; Bannerji, R. New analytical stellar model in general relativity. *Phys.Rev. D27*. 1983, 328-331.
44. Ngubelanga, S.A., Maharaj, S.D. and Ray, S. (2015). Compact stars with linear equation of state in isotropic coordinates. *Astrophys. Space.Sci.* 357, 40

Citation: Fahim A. Shaltout, "Impact of Preservatives on Food Preservation and their Effect on the Bacteria", *Universal Library of Innovative Research and Studies*, 2024; 1(2): 01-08. DOI: <https://doi.org/10.70315/uloap.ulirs.2024.0102001>.

Copyright: © 2024 The Author(s). This is an open access article distributed under the Creative Commons Attribution License, which permits unrestricted use, distribution, and reproduction in any medium, provided the original work is properly cited.